Vector Alignment and Dimensionality in Turbulence

A. Noullez

Vector Alignment and Dimensionality in Turbulence

A. Noullez*
Université Côte d'Azur, Observatoire de la Côte d'Azur, CNRS, Laboratoire Lagrange, bd. de l'Observatoire, C.S. 34229, 06304 Nice Cedex 4, France
(Dated: May 19, 2025)

Rapid local directional alignment of different vector quantities has been observed in incompressible turbulence, either in MHD or in fluid turbulence, in both direct numerical simulations or in Solar wind data, and these alignments weaken the nonlinear terms with respect to those expected for Gaussian independent random fields. Evidence are based on the comparison of the probability distributions of the angle between vectors to the one expected for independent isotropic three-dimensional vectors. We show that this apparent alignment can also be attributed to a local anisotropic reduction of the dimensionality of the structures towards bidimensionality, leading to an increased probability of finding vectors close to alignment, compared to the spatial three-dimensional case. This interpretation is checked numerically and in Helios-2 Fast and Slow Solar wind data.

I. INTRODUCTION

It has long been observed that different vector fields of turbulence show intriguing alignment or antialignment. This is the case for velocity $\boldsymbol{v}$ and vorticity $\boldsymbol{\omega} \equiv \boldsymbol{\nabla}\times\boldsymbol{v}$ in hydrodynamic turbulence [1–3], but also appears for velocity $\boldsymbol{v}$ and magnetic field $\boldsymbol{b}$ [4–9], magnetic field $\boldsymbol{b}$ and current $\boldsymbol{j} \equiv \boldsymbol{\nabla}\times\boldsymbol{b}$, or current $\boldsymbol{j}$ and vorticity $\boldsymbol{\omega}$ in MHD turbulence [10, 11], with measurements both in numerical simulations of decaying MHD turbulence [8, 9], or *in-situ* observations in the Solar wind [4–7, 9, 11, 12]. Of course, all of these vector fields are physically coupled in turbulence, and we should *not* expect them to be independent and uncorrelated, without any specific tendency towards alignment or orthogonality. But there is no obvious physical explanation of why the dynamics *always* favors alignment or antialignment, and simple models for the dynamics of alignment [3, 8] have been unconclusive till now. Also, these alignments were initially thought to be a slow relaxation process requiring many nonlinear eddy turnover times to drive the turbulent system towards globally aligned Beltrami and/or Alfvénic states that were studied and interpreted as such in [3] or [8], but it has been shown recently that *local* pointwise directional alignment also occurs in fluid or MHD turbulence [8–12] and is a fast process, needing less than one eddy turnover time to align vectors in near-independent spatially extended spatial patches. Alignment is dynamically important because it will inhibit the nonlinear terms in the corresponding hydrodynamical equation [3, 13], and slow down the dynamics with respect to what would be expected of random fields.

The main diagnostic to evidence these alignment or antialignment effects is the computation of the probability density functions (PDFs) of the local angle cosine between the two vector fields $\boldsymbol{f}$ and $\boldsymbol{g}$

$$c \equiv \cos\theta = \frac{\boldsymbol{f}\cdot\boldsymbol{g}}{|\boldsymbol{f}|\,|\boldsymbol{g}|} \ , \tag{1}$$

where $\boldsymbol{f}$ and $\boldsymbol{g}$ can be $\boldsymbol{v}$ and $\boldsymbol{\omega}$ in neutral fluid turbulence, or $\boldsymbol{v}$ and $\boldsymbol{b}$, $\boldsymbol{j}$ and $\boldsymbol{b}$, or $\boldsymbol{j}$ and $\boldsymbol{\omega}$ in MHD turbulence. Compared to a uniform distribution often presented without justification as the one expected for Gaussian uncorrelated vectors, these PDFs are found to become strongly peaked around $c \approx \pm 1$ (aligned vectors) and depleted for $c \sim 0$ (orthogonal vectors). In this paper, we show that a flat $\cos\theta$ distribution is *not* a signature of Gaussianity, and will occur for any probability distribution of the vector components, but only in the case of independent isotropic three-dimensional vectors, and breaking *any* of these three conditions will produce of a departure of the uniform distribution. Moreover, for three-dimensional vectors, any anisotropy common to the two vector fields will induce a reduced dimensionality of the vectors and produce an apparent local directional alignment, even if the vectors are not necessarily preferentially oriented along a common line, but maybe in a common (hyper)plane. We emphasize that the dynamical alignment effect remains a true feature of turbulence, but its geometrical interpretation and visualization should be done carefully, as already vectors in a plane have a higher probability of alignment than vectors in space.

II. ANGLE PDFS FOR RANDOM VECTORS

We now derive analytically the PDF $p_d(\theta)$ of the angle θ between random vectors in any space dimension d. The goal here is not to compute its value for arbitrarily large or non-integer dimensions, but rather to show that it depends continuously on the dimension and that alignment is *always* favored in lower dimensions. Its expression can be obtained analytically for the special case of isotropic $\langle f_\alpha f_\beta\rangle = \langle g_\alpha g_\beta\rangle = \delta_{\alpha,\beta}$ and independent $\langle f_\alpha g_\beta\rangle = 0$ vectors with components f_α, g_β and space dimensions $\alpha, \beta = 1, \ldots, d$, the mean $\langle\cdot\rangle$ being over all possible realizations of the vectors. These conditions then mean that this PDF will be *universal* with respect to the distribution of the vectors components magnitude, and so the Gaussian hypothesis is not needed, as the angle between vectors Eq. (1) does not depend on their

* anz@oca.eu

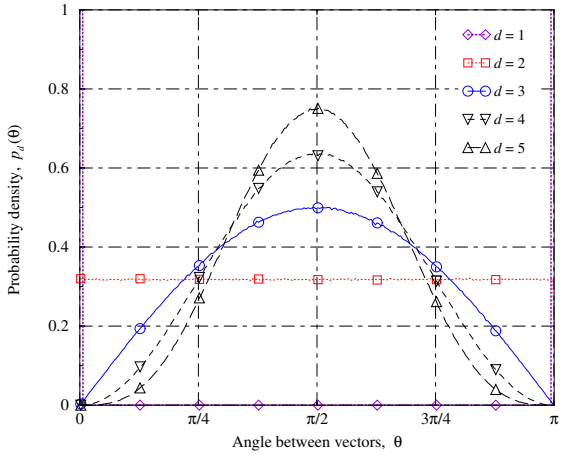

FIG. 1. PDFs of the angle θ between random independent isotropic vectors for spatial dimensions $d = 1$ to $d = 5$.

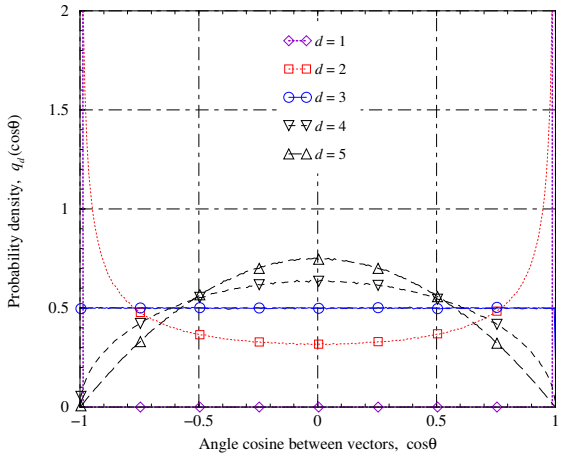

FIG. 2. PDFs of the angle cosine $\cos\theta$ between random independent isotropic vectors for spatial dimensions $d = 1$ to $d = 5$.

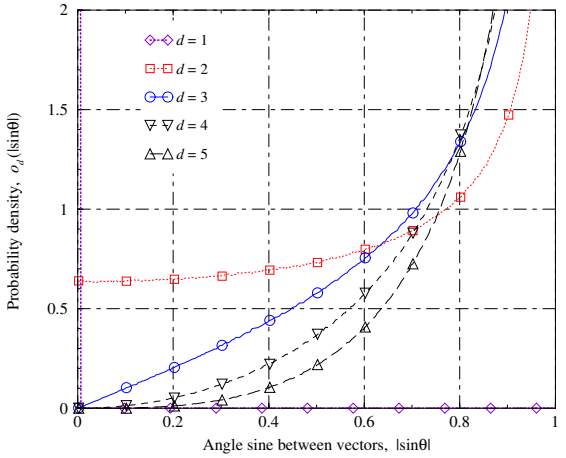

FIG. 3. PDFs of the angle sine $|\sin\theta|$ between random independent isotropic vectors for spatial dimensions $d = 1$ to $d = 5$.

length. The isotropy and independence properties then imply that the distribution of the intersection of the second vector direction on the d-dimensional sphere is uniform if the first vector direction is fixed. Using a uniform parametrization of the hypersphere with $d-1$ angles like in [14], and integrating over $d-2$ angles gives the sought distribution of the remaining angle θ

$$p_d(\theta) = \frac{\Gamma\left(\frac{d}{2}\right)}{\sqrt{\pi}\,\Gamma\left(\frac{d-1}{2}\right)}\,(\sin\theta)^{d-2}\ , \tag{2}$$

shown in Fig. 1, and by a change of variable, the PDF $q_d(c)$ of the angle cosine c

$$q_d(c) = \frac{p_d(\theta)}{|\sin\theta|} = \frac{\Gamma\left(\frac{d}{2}\right)}{\sqrt{\pi}\,\Gamma\left(\frac{d-1}{2}\right)}\left(1-c^2\right)^{(d-3)/2} \tag{3}$$

shown in Fig. 2. PDFs $o_d(s)$ of $s \equiv |\sin\theta| = |\boldsymbol{f}\times\boldsymbol{g}|/(|\boldsymbol{f}|\,|\boldsymbol{g}|)$ (the sign of s is not a relevant physical quantity as it depends on the orientation of the reference frame) can be computed again by a simple change of variable to obtain

$$\begin{aligned} o_d(s) &= \frac{2\,p_d(\theta)}{|\cos\theta|} = 2\,q_d(c)\,|\tan\theta| \\ &= \frac{2\,\Gamma\left(\frac{d}{2}\right)}{\sqrt{\pi}\,\Gamma\left(\frac{d-1}{2}\right)}\ \frac{s^{d-2}}{\sqrt{1-s^2}}\ . \end{aligned} \tag{4}$$

$q_d(c)$ and $p_d(\theta)$ cannot be both uniform (and $o_d(s)$ never is) and it is a coincidence that $p_2(\theta) = 1/\pi$ is uniform in 2-d and $q_3(c) = 1/2$ uniform in 3-d. In high dimensions, vectors have a higher probability of being close to orthogonal, while in lower dimensions vectors display a tendency for alignment and the PDF $q_d(c)$ becomes peaked near $c \approx \pm 1$ for $d < 3$, even if the vectors are independent. In one dimension, vectors become trivially aligned, and $q_1(c)$ consists of two delta functions at $c = \pm 1$, while $o_1(s)$ is a delta function at $s = 0$.

This tendency towards alignment can be quantified in various ways, the simplest being to compute the moments of these PDFs. By symmetry, we have that $\langle\theta\rangle = \pi/2$ and $\langle\cos\theta\rangle = \langle\sin\theta\rangle = 0$, so that the corresponding variances $\mathrm{Var}(\theta) \equiv \langle(\theta - \langle\theta\rangle)^2\rangle$ and $\mathrm{Var}(\cos\theta) = \langle\cos^2\theta\rangle = 1 - \langle\sin^2\theta\rangle$ (found to be exactly equal to $1/d$) are a measure of alignment and, as Fig. 4 show, increase continuously and monotonically with decreasing dimensions. Other measures of alignment are the mean values of the angle cosine absolute value $\langle|\cos\theta|\rangle$ and the (complemented) angle sine absolute value $\langle 1 - |\sin\theta|\rangle$ that can also be computed explicitly and are displayed in Fig. 4, going from 1 (perfect alignment for $d = 1$) towards zero (near sure orthogonality) for high dimensions. This property is crucial to understand that the expected mean value of nonlinear terms $|\boldsymbol{f}\times\boldsymbol{g}|$ (normalized by $|\boldsymbol{f}|\,|\boldsymbol{g}|$) will be reduced from the value predicted for d-dimensional random vectors if the dynamics drives the vectors on a lower dimension manifold (for instance, $\langle|\cos\theta|\rangle$ goes from 0.5 to 0.64 and $\langle|\sin\theta|\rangle$ from 0.79

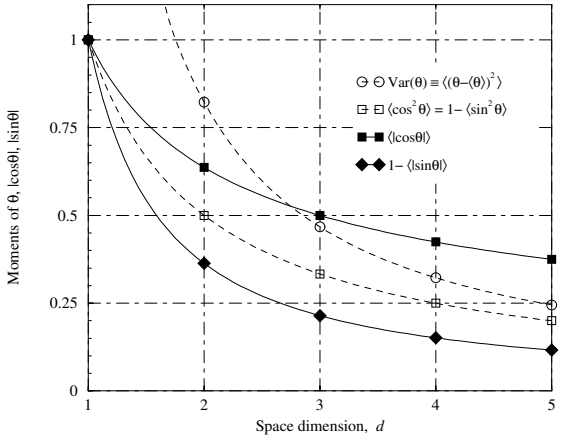

FIG. 4. Variances (dashed lines, empty symbols) and mean absolute values (continuous lines, full symbols) for the angle θ, the angle cosine $|\cos\theta|$ and the (complemented) angle sine $|\sin\theta|$ between random independent isotropic vectors for spatial dimensions $d = 1$ to $d = 5$, showing the monotonic tendency towards alignment for lower dimensions.

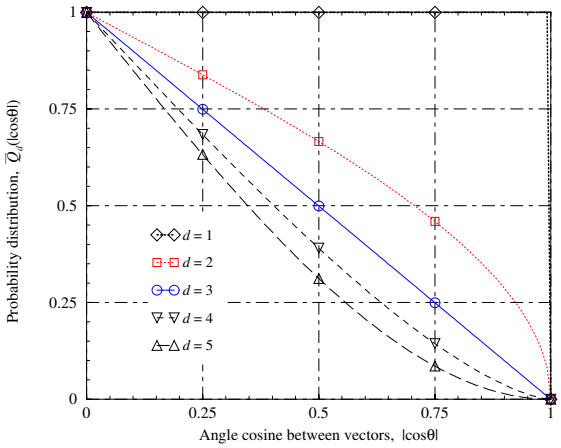

FIG. 5. Probabilities (cumulated PDFs) $\overline{Q}_d(c) \equiv \mathcal{P}(|\cos\theta| \geq c)$ of higher alignment for spatial dimensions $d = 1$ to $d = 5$, showing that these probabilities are always larger for decreasing dimensions and at any value of c, indicating the higher probability of alignment or antialignment ($|\cos\theta| \approx 1$) of random independent isotropic vectors in lower dimensions.

to 0.64 when going from $d = 3$ to $d = 2$). As we show later in section IV, the same effect occurs if the dynamics induces an anisotropy shared by the two vectors $\boldsymbol{f}$ and $\boldsymbol{g}$.

This alignment effect can also be quantified by computing probabilities of alignment $\overline{Q}_d(c) \equiv \mathcal{P}(|\cos\theta| \geq c) = \overline{P}_d(a \equiv \arccos c) \equiv \mathcal{P}(|\theta - \pi/2| \geq a)$, as these PDFs can be integrated for integer dimensions to obtain probability distributions, and Fig. 5 show that this probability of alignment is everywhere larger for lower dimensions. For instance, we have $\overline{Q}_2(c) = 2/\pi \arccos c \geq \overline{Q}_3(c) = 1 - c$ (substitute $c \equiv \cos a$ to obtain $2\,P_d(a) \equiv 2\,\mathcal{P}(\theta < a)$, so that $P_2(a) = a/\pi \geq P_3(a) = (1 - \cos a)/2 = \sin^2(a/2)$). Near-alignment is thus significantly more probable in 2-d than it is in 3-d, and Fig. 6 of [8] showing aligned patches in a 2-d simulation is misleading as already random vectors have a 50 % probability of having $|\cos\theta| \geq 0.7$ in 2-d while it would be only 30 % in 3-d. This increased alignment is *not* an artefact of looking at PDFs of $\cos\theta$ instead of those of θ, as random vectors have a 50 % probability of having $\theta < \pi/4$ or $\theta > 3\pi/4$ in 2-d, while it is only 30 % in 3-d.

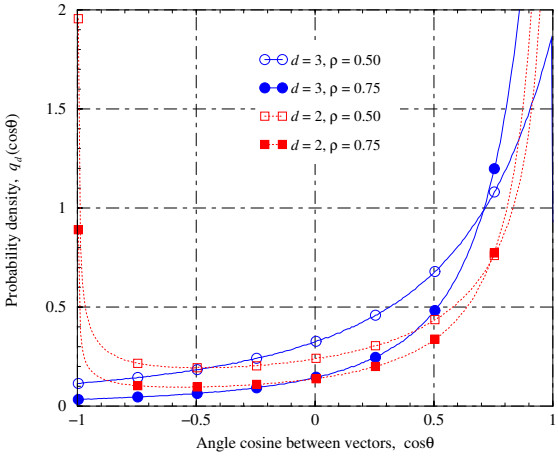

FIG. 6. PDF of the angle cosine $\cos\theta$ between random Gaussian correlated isotropic vectors for $\rho = 0.5$ (empty symbols) and $\rho = 0.75$ (full symbols) and space dimensions $d = 3$ (circles) and $d = 2$ (squares).

III. CORRELATED RANDOM VECTORS

We now check if the alignment induced by a reduction of the vector dimensionality persists if the vectors are correlated. In that case, there is no general analytic result for PDFs of the angle, and for nonzero value of the correlation coefficient

$$\rho = \frac{\langle \boldsymbol{f} \cdot \boldsymbol{g} \rangle}{\sqrt{\langle |\boldsymbol{f}|^2 \rangle \, \langle |\boldsymbol{g}|^2 \rangle}} \,, \tag{5}$$

the PDF depends on ρ, and thus will be different for different distributions of the vectors components magnitude. We can however resort to numerical simulations to compute PDFs for the special case of correlated Gaussian vectors by generating independent Gaussian isotropic vectors $\boldsymbol{f}$ and $\boldsymbol{h}$ and then computing

$$\boldsymbol{g} = \rho\, \boldsymbol{f} + \sqrt{1 - \rho^2}\, \boldsymbol{h} \,, \tag{6}$$

that will be Gaussian, isotropic and correlated with $\boldsymbol{f}$: $\langle f_\alpha g_\beta \rangle = \rho\, \delta_{\alpha,\beta}$ (see [15] for details), and then looking at the PDF of Eq. (1), shown in Fig. 6 for different values of d and ρ. Only positive values of the correlation ρ are considered as changing the correlation sign would simply favor antialignment rather than alignment of $\boldsymbol{f}$ and $\boldsymbol{g}$ and mirror left-right the PDF $q_d(c)$ of the angle cosine c. The main characteristics of the isotropic PDFs are preserved,

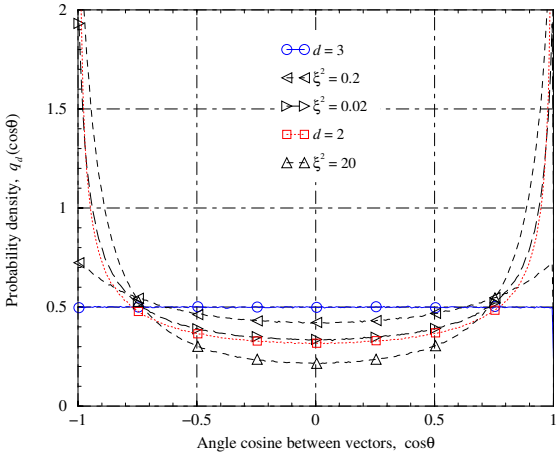

FIG. 7. PDF of the angle cosine $\cos\theta$ between random independent anisotropic three-dimensional vectors for different anisotropic amplitudes $\xi^2 = \langle f_1 f_1 \rangle = \langle g_1 g_1 \rangle$. Isotropic distributions for $d = 3$ (corresponding to $\xi^2 = 1$) and $d = 2$ (corresponding to $\xi^2 = 0$) are shown for comparison. The bottom case $\xi^2 = 20 \gg 1$ displays strong alignment, larger than for isotropic 2-d vectors and close to 1-d isotropic random vectors.

that is $q_3(c)$ goes to finite values for both $c = \pm 1$ even for strong values of ρ, while the 2-d PDF $q_2(c)$ still diverges and becomes larger than $q_3(c)$ for $c \to \pm 1$ but is always flatter than $q_3(c)$ around the orthogonal direction $c \sim 0$.

IV. ANISOTROPIC RANDOM VECTORS

We now ascertain that anisotropy in the random vectors distribution can induce a reduction in the vectors dimensionality and thus an apparent alignment of the vectors even if the anisotropy is not purely unidimensional. We generate numerically independent random Gaussian 3-d vectors, with a variance depending on the direction : ξ^2 in direction 1 and unity in the others, for both vectors

$$\langle f_\alpha f_\beta \rangle = \langle g_\alpha g_\beta \rangle = \delta_{\alpha,\beta} \left[\xi^2 \delta_{\alpha,1} + (1 - \delta_{\alpha,1}) \right] . \qquad (7)$$

If $\xi^2 > 1$, the anisotropy is one-dimensional, with the two vectors pointing preferentially in direction 1, and trivially aligning together in that direction, with a PDF $q(c)$ tending for $\xi^2 \gg 1$ to the one for 1-d isotropic vectors (two delta functions at $c = \pm 1$), see the bottom curve of Fig. 7. Less obviously, if $\xi^2 < 1$, the anisotropy is two-dimensional, with the vectors lying preferentially in the 2,3-plane, but there is still an apparent alignment of the two vectors with respect to the 3-d isotropic case, due to the reduced probability of orthogonality and the increased probability of alignment, with the PDF $q(c)$ changing continuously from the 3-d isotropic form to the 2-d one when ξ^2 goes from one to zero (see again Fig. 7). For small values of ξ^2, the PDF for 3-d anisotropic vectors is nearly identical to the one for 2-d isotropic ones, and it is only very close to alignment $c \approx \pm 1$ that they can be distinguished. Once more, the degree of alignment (as measured for instance by $\langle \cos^2 \theta \rangle$) increases monotonically with the anisotropy strength $1/\xi^2$. This alignment occurs even though vectors $\boldsymbol{f}$ and $\boldsymbol{g}$ are *uncorrelated* and in fact point uniformly in any direction in the 2,3-plane, but is a pure geometrical effect of the vectors sharing preferentially a common plane (but not a common direction). Indeed, it must be stressed that this alignment completely disappears and the PDF $q(c)$ is the 3-d isotropic one if the anisotropic direction(s) are not the same for $\boldsymbol{f}$ and $\boldsymbol{g}$. On the other hand, if the anisotropies are in the same direction(s), both one- ($\xi^2 > 1$) and two-dimensional ($\xi^2 < 1$) anisotropy will lead to an apparent alignment in 3-d.

V. SOLAR WIND OBSERVATIONS

We check these results in Solar wind data, using the measurements obtained by the Helios-2 spacecraft during the year 1976. These measurements have been extensively studied [5, 6, 16] and are of a good quality, having been obtained during a Solar minimum. Also, they were for a long time the only data showing the evolution of Solar wind turbulence as the spacecraft moved from a distance of 0.9 AU around day 45 of 1976, down to 0.3 AU around day 110 of 1976. We use data sampled at 81 s time resolution to have simultaneous measurements of the 3 components of the velocity $\boldsymbol{v}$ and magnetic field $\boldsymbol{b}$ expressed in the RTN reference frame (see [16] for definitions), where the R (radial) component points away from the Sun and is nearly aligned with the mean velocity and mean advected Solar magnetic field. Moving on the ecliptic, Helios-2 encountered both Fast and Slow Solar wind streams, known to have different origins and physical properties [16]. To explore different physical situations and ensure statistical stationarity in each dataset, we analyzed independently three Slow streams (recognized by $|\boldsymbol{v}| \ll 500\,\mathrm{km/s}$), namely 1976:46–48, 1976:72–74 and 1976:98–101, and three Fast streams ($|\boldsymbol{v}| \gg 500\,\mathrm{km/s}$), 1976:49–52, 1976:76–78 and 1976:105–108. These datasets are 2–3 days long (≈ 3000 points) and avoid streams edges and boundaries. In each of these streams, we remove the fields means (obtained by time-averaging $\overline{\cdot}$ over the full stream lengths), build the field fluctuations $\delta\boldsymbol{v}(t) \equiv \boldsymbol{v}(t) - \overline{\boldsymbol{v}}$ and $\delta\boldsymbol{b}(t) \equiv \boldsymbol{b}(t) - \overline{\boldsymbol{b}}$ and construct the local instantaneous angle

$$\cos\theta(t) = \frac{\delta\boldsymbol{v}(t) \cdot \delta\boldsymbol{b}(t)}{|\delta\boldsymbol{v}(t)|\,|\delta\boldsymbol{b}(t)|} . \qquad (8)$$

Fig. 8 shows an example time series of $\cos\theta(t)$ for the Fast stream 1976:105–108, showing that the wind is strongly Alfvénic, consisting mostly of outward propagating waves with $\delta\boldsymbol{b}$ nearly antiparallel to $\delta\boldsymbol{v}$. This is true for all of the Fast streams encountered at this heliospheric distance, while the encountered Slow streams can display both positive or negative cross-helicity (correlation), but of weaker magnitude. As the left part of Fig. 9 shows,

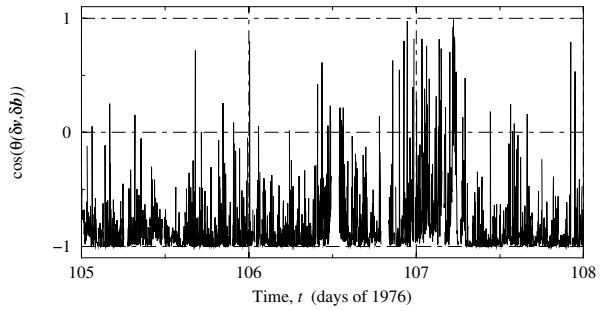

FIG. 8. Time series of the cosine of the instantaneous angle between velocity fluctuations $\delta\boldsymbol{v}$ and magnetic fluctuations $\delta\boldsymbol{b}$ in a Solar wind Fast Stream recorded by the Helios-2 satellite between days 105 and 108 of the year 1976, showing the strong negative cross-helicity (anti-alignment) of $\delta\boldsymbol{v}$ and $\delta\boldsymbol{b}$.

streams with opposite signs of the correlation between $\delta\boldsymbol{v}$ and $\delta\boldsymbol{b}$ but similar correlation magnitude simply mirror left-right the PDF of the angle cosine and exchange the preferences of aligned or antialigned vectors, but without changing the overall PDF shape except for the left-right symmetry, an effect already observed in the work of [9].

The PDFs of $\cos\theta(t)$ for the three Slow and three Fast wind streams are shown together in Fig. 9, and one can notice that they differ significantly. PDFs for Slow streams are very similar to those for 3-d correlated isotropic random vectors (Fig. 6), while those for Fast wind streams are much more strongly aligned. We now check that this alignment can be attributed to an increased anisotropy and corresponding reduced dimensionality of the $\delta\boldsymbol{v}$ and $\delta\boldsymbol{b}$ fields by computing the cross-correlation matrix $\langle \delta\boldsymbol{v}\, \delta\boldsymbol{b}^{\boldsymbol{T}} \rangle / \sqrt{\langle|\delta\boldsymbol{v}|^2\rangle\, \langle|\delta\boldsymbol{b}|^2\rangle}$. In the Fast stream 1976:105–108, its value is

$$\overline{\delta v_\alpha\, \delta b_\beta} = \begin{pmatrix} -0.15 & -2\times10^{-3} & 6\times10^{-2} \\ -2\times10^{-2} & -0.34 & -7\times10^{-3} \\ 4\times10^{-2} & -7\times10^{-3} & -0.39 \end{pmatrix} , \quad (9)$$

with similar values for the other Fast streams, and is dominated by the T and N components, suggesting a 2-d anisotropy, a feature already observed by various authors [4, 5]. To verify that this anisotropy is associated to the nature of the stream, we compute the components local variances $\overline{\delta {b_\alpha}^2}\,(t) \equiv \overline{(b_\alpha - \overline{b_\alpha})^2}\,(t)$, where the time average $\overline{\cdot}(t)$ is now defined as an 8 hours moving average centered on t. The resulting Fig. 10 shows that there is an abrupt change in the components local variances, associated with strong inhomogeneities at the stream boundaries, when switching from Slow stream 1976:98–101 to the Fast stream 1976:105–108. While the three components local variances are nearly identical in the Slow stream, the transverse local variances increase by a factor ~ 3 in the Fast stream, and both fields $\delta\boldsymbol{b}$ and $\delta\boldsymbol{v}$ (the latter not shown in Fig. 10) become anisotropic with stronger fluctuations in the plane transverse to the R (radial) direction associated to the mean magnetic field $\overline{\boldsymbol{b}}$ and mean velocity $\overline{\boldsymbol{v}}$. As pointed out in the previous section, this Fast wind bidimensionalization increases the apparent 3-d alignment of the two vector fields. However, field fluctuations $\delta\boldsymbol{v}$ and $\delta\boldsymbol{b}$ have very strong Alfvénic (anti)correlations in *all* components, and so the T and N components remain correlated and display an angle PDF corresponding to a strong (anti)alignment between $\delta\boldsymbol{v}$ and $\delta\boldsymbol{b}$ in the T, N-plane with asymmetric PDFs skewed towards $\cos\theta \approx -1$, $\theta \approx \pi$, this time due to the (anti)correlation $\rho \simeq -1$.

VI. DISCUSSION AND CONCLUSIONS

The image of aligned vectors that comes naturally to mind is that of vectors that point towards close or nearly opposite directions. But two random vector fields in (hyper)space will also display a higher probability of mutual alignment with respect to the isotropic distribution, if they have been dynamically pushed on a lower dimensional (hyper)plane rather than on a line, even if the two fields have no particular alignment in this plane. The effect is completely geometrical and comes from the decreased probability of orthogonality and increased likelihood of alignment when reducing the dimension or increasing the anisotropy of the two vector fields. This distinction between linear and planar alignment might seem purely semantic, as lying in a common plane *is* some kind of alignment between the vectors. Also, the dynamical consequences like the reduction of nonlinearity due to decreased values of $\boldsymbol{f}\times\boldsymbol{g}$ and increased values of $\boldsymbol{f}\cdot\boldsymbol{g}$ remain the same and do not depend on that interpretation. It is however important to realize and understand if the structures that appear locally in 3-d fluid or MHD turbulence are preferentially lines or sheets, and we showed that only analyzing the PDFs of $\cos\theta$ cannot completely distinguish or exclude the two possibilities, as both types of structures will show an alignment of the vectors. The alignment of different vector fields however does not allow to make any particular prediction about the *spatial* structure of each field, like the spectrum or the structure functions. But it implies some *local* properties of the fields correlations that have important dynamical consequences. For instance, the results in section IV show that any 2-d anisotropy shared by the fields will lead to alignment and Beltramization, with a corresponding slowdown of the dynamics because of the reduction of $|\sin\theta|$ and a greater probability of observation of these local states, and this mechanism could be a possible explanation of the paradox of the predominance of highly Alfvénic states in plasma turbulence [13], with immediate consequences on the power spectra to favor a Kraichnan spectrum instead of a Kolmogorov spectrum (see again [13]). In fluid turbulence, the main effect will be an increase of the characteristic times for the energy transfer along scales in the turbulent cascade.

But complete dynamical local alignment of any type won't occur over the whole of space, and it has been shown in [8–11] that it occurs in extended spatial patches

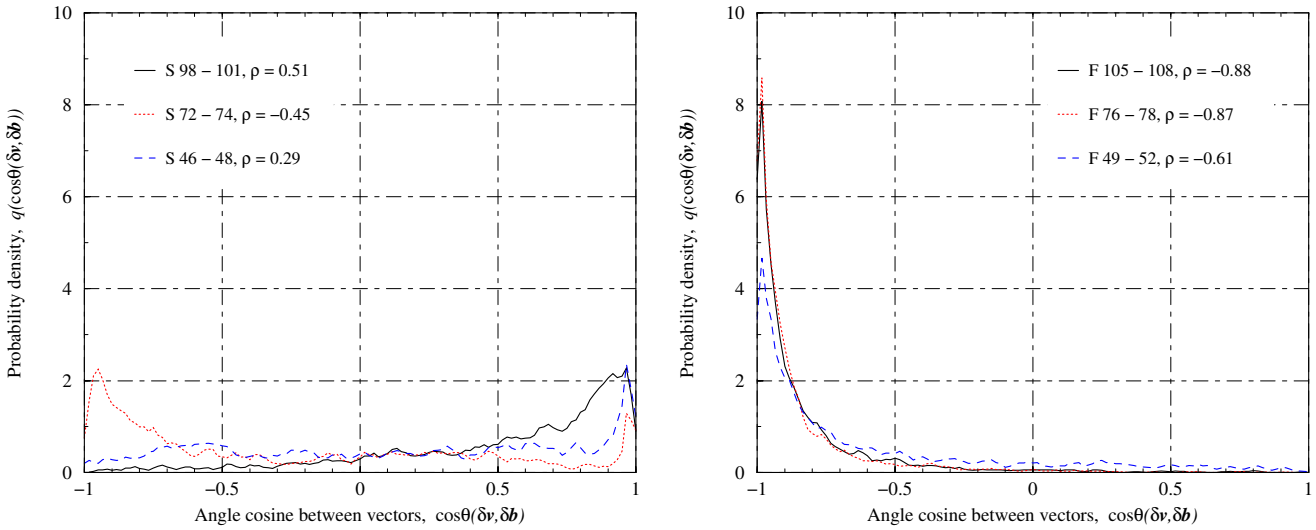

FIG. 9. PDFs of the angle cosine $\cos\theta$ between velocity $\delta\boldsymbol{v}$ and magnetic fluctuations $\delta\boldsymbol{b}$ in three Solar wind Slow Streams (left) and three Fast Streams (right), at the same scale. Reversing the cross-helicity sign would mirror the PDFs.

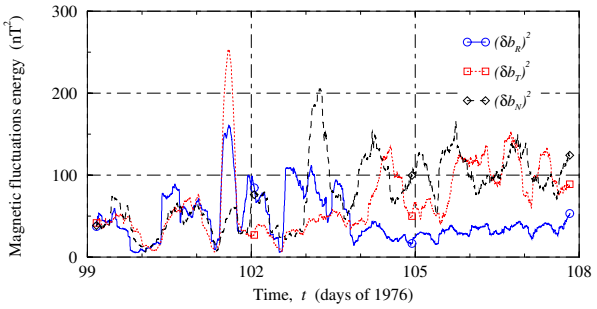

FIG. 10. Time series of of the magnetic fluctuation $\delta\boldsymbol{b}$ components local energy $\overline{\delta b_\alpha{}^2}$. Note the increased energy by a factor ~ 3 of the components transverse to the radial direction (corresponding to the mean magnetic field), when switching from a Slow ($t \leq 101$) to a Fast ($t \geq 104$) Stream around the streams edge boundary $t \approx 102$.

displaying local alignment or antialignment. The situation is easier and the analysis is simpler in the Solar wind as the radial expansion of the wind and the advected mean magnetic field create a constant direction in which the fluctuations are reduced, so that the anisotropy is 2-d with a preserved direction. In homogenous fluid or MHD turbulence, the situation is more complex but the spectra of both $\boldsymbol{v}$ and $\boldsymbol{b}$ are IR-divergent, that is completely dominated by the large scales, so we can expect that the local slow large-scale field can dynamically induce 2-d or 1-d local anisotropy and a local directional alignment or antialignment, with a slow time evolution and spatially varying direction. PDFs of $\cos\theta$ will in that case be a mixture of different situations similar to those shown in Fig. 6 and Fig. 7 as neither the correlation ρ nor the anisotropy will be uniform, but PDFs will in any case display alignment of the vector fields if anisotropies of both fields are similarly oriented. It is interesting to note that it has been observed in the solar wind [17] that anisotropy in the magnetic field is strongly bidimensional, but also changes shape continuously with scales. We can thus expect that alignment will also vary with the considered scale and we plan to tudy this effect in a future work.

Also, PDFs of $\cos\theta$ can give a hint of the shape and dimension of structures that are effectively present at various scales in the vector fields. For example, $\langle\cos^2\theta\rangle = 1/d$ for isotropic independent vectors (this result is modified if vectors are correlated), and this defines a kind of "effective dimension" for isotropic or anisotropic vector fields, and PDFs shown in Fig. 7 will have a value of $1/\langle\cos^2\theta\rangle$ that changes continuously from 3 to 2 for increasing 2-d anisotropies and down to 1 for increasing 1-d anisotropy.

Finally, we want to stress again that Gaussianity does not explain and is neither a necessary nor sufficient condition to ensure the absence of alignment effects, unless considering the restricted definition of homogeneous and isotropic Gaussian field for which any linear operator acting on it produces an isotropic Gaussian variable, and the considered fields are independent. We have shown that fields that only have Gaussian components but that are not independent and isotropic can lead to alignment of vector fields, while independent, homogeneous and isotropic fields cannot produce alignment effects, even if they don't have Gaussian components. The procedure of randomizing the phases of the Fourier transform of vector fields, that is used for instance in [9], indeed produces the restricted form of a Gaussian field, in which all components of the vectors or any combination of them is a Gaussian variable, but this is a side effect, while the main consequence of the procedure is to produce homogeneous, isotropic and independent fields (see e.g. [18]), thus breaking any alignment possibility.

We conclude that local or global vectors alignment is a *geometrical* property that depends on the vectors dimensionality or anisotropy, and that it is favored in low dimensions or strong anistotropy. So, if the dynamics drive the vectors on a lower dimensional or anisotropic variety, the vectors will appear more aligned than if they span the whole space directions. This increased alignment is a real effect, even if the vectors do not necessarily point along the same line, and its consequences on the dynamics through a reduction of the nonlinearity and a slowdown of the nonlinear transfers are also real, so that these aligned anisotropic states will also enjoy a higher probability of being observed once they are realized.

ACKNOWLEDGMENTS

It is a pleasure to thank A. Pouquet, R. Bruno, and L. Sorriso-Valvo for many useful discussions, comments, suggestions and insights on the properties of MHD turbulence and on the many traps and pitfalls lurking in the processing and analysis of Solar wind data.

[1] R.B. Pelz, V. Yakhot, S.A. Orszag, L. Shtilman, and E. Levich, Phys. Rev. Lett. **54**, 2505 (1985). I
[2] R.M. Kerr, Phys. Rev. Lett. **59**, 783 (1987).
[3] R.H. Kraichnan and R. Panda, Phys. Fluids **31**, 2395 (1988). I
[4] J.W. Belcher and L. Davis, Jr., J. Geophys. Res. **76**, 3534 (1971). I, V
[5] B. Bavassano, M. Dobrowolny, G. Fanfoni, F. Mariani, and N.F. Ness, Sol. Phys. **78**, 373 (1982). V, V
[6] D.A. Roberts, M.L. Goldstein, L.W. Klein, and W.H. Matthaeus, J. Geophys. Res. **92**, 12023 (1987). V
[7] J.J. Podesta, B.D.G. Chandran, A. Bhattacharjee, D.A. Roberts, and M.L. Goldstein, J. Geophys. Res. **114**, A01107 (2009). I
[8] W.H. Matthaeus, A. Pouquet, P.D. Mininni, P. Dmitruk, and B. Breech, Phys. Rev. Lett. **100**, 085003 (2008). I, II, VI
[9] K.T. Osman, M. Wan, W.H. Matthaeus, B. Breech, and S. Oughton, Astrophys. J. **741**, 75 (2011). I, V, VI
[10] S. Servidio, W.H. Matthaeus, and P. Dmitruk, Phys. Rev. Lett. **100**, 095005 (2008). I
[11] S. Servidio, C. Gurgiolo, V. Carbone, and M.L. Goldstein, Astrophys. J. **789**, L44 (2014). I, VI
[12] W.H. Matthaeus, M. Wan, S. Servidio, A. Greco, K.T. Osman, S. Oughton, and P. Dmitruk, Phil. Trans. R. Soc. A **373**, 20140154 (2015). I
[13] M. Dobrowolny, A. Mangeney, and P. Veltri, Phys. Rev. Lett. **45**, 144 (1980). I, VI
[14] S. Degerine, Ann. Inst. Henri Poincaré **XV-1**, 63 (1979). II
[15] D.E. Knuth, *The Art of Computer Programming, Vol. 2: Seminumerical Algorithms*, (Addison-Wesley, Boston, 3rd. edition, 1997). III
[16] R. Bruno and V. Carbone, Living Rev. Sol. Phys. **10**, 2 (2013) ; R. Bruno and V. Carbone, *Turbulence in the Solar Wind*, (Springer Lecture Notes in Physics, Springer, Switzerland, 2016). V
[17] C.H.K. Chen, A. Mallet, A.A. Schekochihin, T.S. Horbury, R.T. Wicks, and S.B. Bale, Astrophys. J. **758**, 120 (2012). VI
[18] A. Papoulis, *Probability, Random Variables, and Stochastic Processes*, (McGraw-Hill, New York, 3rd. edition, 1997). VI